Kuznetsov, Aleksandr D.; Holopainen, Jari; Viikari, Ville

Optimization of Loads for Antenna-Based Scattering Systems Using Feedforward Neural Networks

Published in:
18th European Conference on Antennas and Propagation, EuCAP 2024

DOI:
10.23919/EuCAP60739.2024.10501204

Published: 01/01/2024

Document Version
Publisher's PDF, also known as Version of record

Optimization of Loads for Antenna-Based Scattering Systems Using Feedforward Neural Networks

Aleksandr D. Kuznetsov*, Jari Holopainen*, Ville Viikari*,
*Department of Electronics and Nanoengineering, Aalto University, Espoo, Finland, aleksandr.kuznetsov@aalto.fi

***Abstract*—In this paper, we optimize the passive loads of a scattering system consisting of multiple coupled antennas using multi-layer feedforward neural networks. The developed in this study architectures, trained to solve a classification task, predict the load impedance values connected to unit antenna scatterers based on the bistatic radar cross-section of a structure. Trained networks exhibit potential in optimizing load values for scattering redirection among predefined directions. To demonstrate the applicability of the proposed method, two multi-layer feedforward neural networks are trained and used to predict proper load impedances for different scattering objectives. Additionally, existing limitations of the method usage are discussed with the potential ways to mitigate them.**

***Index Terms*—antenna scattering system, neural network, loads optimization, bistatic RCS.**

I. Introduction

Interest in scattering systems has increased in recent years due to their novel applications in communications engineering; for example, in Reconfigurable Intelligent Surfaces and backscattering communication [1], [2]. Depending on the implementation, there are different structural parameters requiring optimization such as structure, materials, and the size of the unit cell. Instead of structural modifications, scattering properties can be also tailored by varying the impedance of loads in the scattering systems composed of antenna-like structures. Theoretical attempts have been made to optimize the load impedance values through their separation from structural parameters, which had limitations with practical implementation [3], [4].

Recently, machine learning algorithms have been used for characterizing scattering properties of complex structures [5], [6] and optimizing of scattering systems for improving its electromagnetic properties [7] or enhancing propagation channels equipped with scatterers [8]. Generally, these approaches partially or totally imply the prediction of the scattering properties of the structure based on its configuration. Existing methods of antenna development utilizing machine learning algorithms (for example, [9], [10]) cannot be directly extrapolated on scattering systems due to the absence of structural scattering influence in radiating antenna development tasks. We are not aware of any machine learning methods that would account for the structural scattering from an antenna system, that is, part of the scattering that does not directly depend on the loads at antenna feeds [11].

In this article, we propose an algorithm to optimize the load impedances connected to antenna elements of the scattering structure using a multi-layer feed-forward neural network (MLFFNN) [12]. Applying supervised learning to solve a classification task, it is shown that MLFFNN may be applied for the prediction of load values based on the bistatic radar cross-section of the structure. Moreover, the paper demonstrates, based on MLFFNN prediction, a possibility to optimize values of loads for increasing radar cross-section in the required direction.

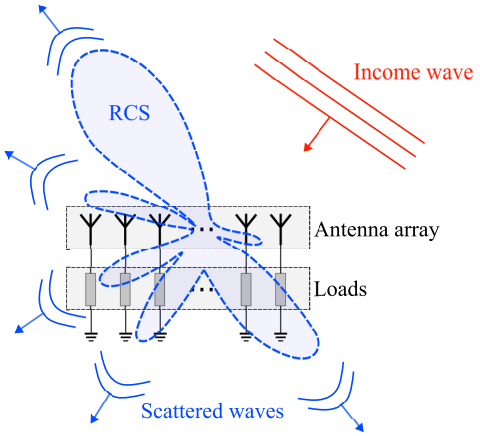

Fig. 1. The general view of an antenna-based scattering system.

II. Methodology

A. Task description

Consider the scattering system based on the antennas loaded with some impedance values (Fig. 1). For general purposes of its application in communications engineering, the characterization of the structure scattering from one to another direction is required. For this purpose, bistatic radar cross-section (RCS) may be applied. In the case of the system under research irradiated by a plane wave coming from some direction, which is a valid assumption for far-field operation region, the distribution of the scattered energy in other directions is described by bistatic RCS for each set of loads connected to antenna ports. Bistatic RCS may be computed theoretically, using simulation, or experimentally. In these terms, the task of this research is to establish the connection between bistatic RCS and load values using MLFFNN trained on the set of known samples which form a dataset. In this research, the dataset was formed based on CST Studio Suite simulations.

The determination of the specific task being researched is essential. It is noteworthy that solving the load values predic-

tion task as a regression involves the complexity of optimizing both the real and imaginary components of load impedances separately. Additionally, engineers often encounter practical implementation challenges when applying the obtained results since they need to generate exactly computed optimal values in a limited space. For these reasons, we have chosen to approach the problem as a classification task, considering the limited range of potential load values explored in this paper.

B. Multi-layer feedforward neural network application

Multi-layer feed-forward neural network (MLFFNN) is a type of artificial neural network (ANN) which has a definite flow of information between layers of neurons [12]. It can operate with several inputs and outputs which allows to apply it to multioutput machine learning tasks. This property is useful for the simultaneous prediction of several parameters, which is applicable to the task under consideration.

In this research, an input layer of MLFFNN is a $N \times 1$ vector which is bistatic RCS (N is a number of scattering directions taken into account) computed for the specific direction of the incoming plane wave for known load values connected to the antennas. The normalization of this vector is not required since it represents the same values for all directions, while the disturbance of the ratio between RCS values in different directions makes no physical sense. An output layer of the structure is a $L \times 1$ vector, whose values represent the class of the load (L is the number of antennas in the system). The architecture of the hidden layers of the neural networks can be changed depending on several factors: N and L values, number of possible classes of loads, available memory resources, etc. The learning of the MLFFNN is supervised: computation of coefficients connecting all neurons between neighbouring layers was based on the pre-computed C sets of bistatic RCS arrays corresponding to C arrays of loads. The utilization of MLFFNN implies the presence of the connection between load impedance values and the overall scattering of the system, demonstrated in [11]. By incorporating a linear combination of outputs from each neuron during the prediction process, MLFFNN effectively captures this dependence. In this context, the deliberate avoidance of a convolution neural network allows to cover all potential connections between scattering in even non-neighbouring directions.

The prediction process itself should include the utilization of the trained neural net which requires $N \times 1$ vector representing the desired scattering pattern. For this aim, the value of the scattering in the desired direction should be maximal. Since in reality the scattering lobes usually cover sectors, it is reasonable to form the $N \times 1$ vector which contains positive values in several neighbouring points to the desired directions and 0 in other directions.

C. Description of the example

To demonstrate the performance of the proposed approach, we considered the scattering system in Fig. 2 which consists of three identical coupled (to contain the generality of the task) near-half-wavelength dipoles made from PEC material. The

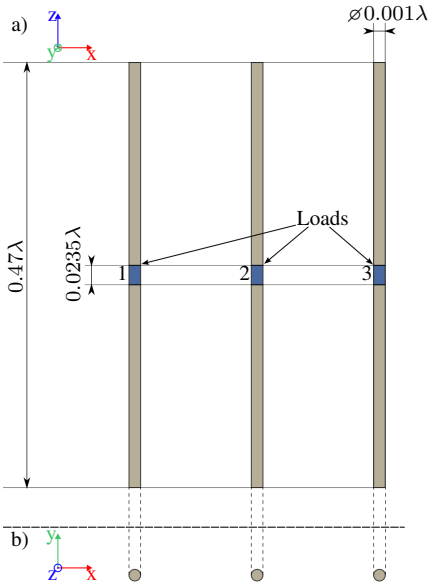

Fig. 2. Back (a) and top (b) view of the structure under test consisting of three dipoles. The sizes are given corresponding to the wavelength at $f = 2.4$ GHz.

TABLE I
THE LIST OF THE PERMITTED LOADS

Type of the load	Values of loads
Resistance (Ω)	short circuit (5 n), 50, open circuit (5 G)
Induction (nH)	0.8, 0.9, 1, 1.2, 1.8, 2, 2.4, 3, 3.5, 4, 5.1
Capacitance (pF)	1, 1.3, 1.5, 1.8, 2, 2.5, 3, 3.5, 4, 4.5, 5, 6, 7, 8

system was under plane wave radiation from $\phi = 40°, \theta = 90°$ direction corresponding to the center of the scattering system in a spherical coordinate system. As possible loads, twenty-eight different impedance values (Table I) were chosen. In Table I loads 5 nΩ and 5 GΩ represent short and open circuits correspondingly. Thus, in this task, we change the bistatic RCS pattern of this structure to form the required shape by varying load values between defined twenty-eight load values.

D. Data preparation

For the training process, the dataset was required. Initially, CST Studio Suite was applied in the process of dataset formation. The dataset initially included 70000 samples, the loads classes for which were pseudo-randomly generated using MATLAB. Since the general number of possible combinations includes only $28^3 = 21952$ permutations with repetitions, there are duplicates in the generated dataset. Thus, all the duplicates were excluded from the dataset which resulted in the presence of 828 non-covered by the provided data combination of loads. It approaches the example task to real tasks in the field. Each sample contained information about bistatic RCS (m^2) computed as a result of scattering of the structure under research terminated to load values vector of whose classes represented the correct answers. Each vector of RCS values contained information about RCS in $N = 684$ different directions with a separation angle equal to 10 degrees

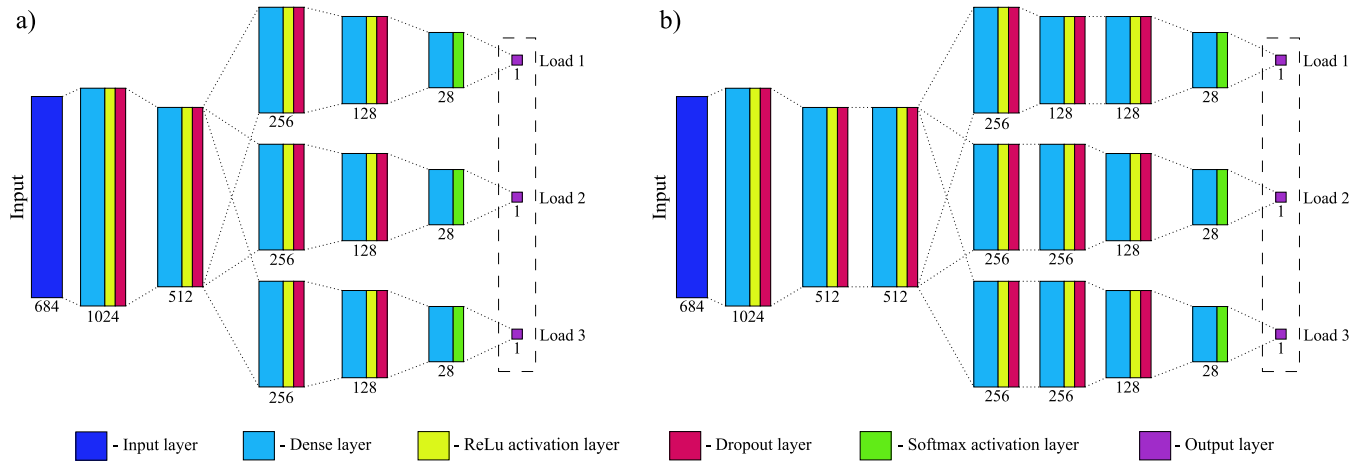

Fig. 3. Architectures of developed and trained MLFFNNs. The number under each layer represents the number of neurons in the layer. Symmetric MLFFNN (a) contains five identical for each branch dense layers before output cells. Modified MLFFNN (b) contains seven dense layers before each output cell and has fewer neurons in the fifth dense layer for the first load branch than in other branches. The result prediction of each MLFFNN is a vector formed by three predicted in each branch value.

between each direction. The whole dataset was separated into train, validation, and test datasets with ratios 0.68:0.12:0.2 ($C_{train} = 14364$, $C_{val} = 2535$, and $C_{test} = 4225$ non-repeating samples correspondingly). To ease the task of the loads determination during the trained network utilisation, all the values were scaled by dividing to the biggest value of RCS in the dataset. Then, during the prediction process, the array of the required values contained 1.4 in the required direction (to cover the possibility that the highest possible RCS value was not achieved in the training dataset), 0.7 in four neighbouring directions, and 0.35 in four neighbouring between the last directions. All the other values in the desired RCS input arrays were equal to 0. As a result, the formed arrays outlined the sector, into which the RCS was desirable while the scattering into other directions was considered as harmful, which allowed us to try to form the required RCS patterns. At the same time, the $L \times 1$ vector of answers, where $L = 3$, was transformed into 3×28 one-hot coded matrix to implement the loss function for MLFFNN training.

III. Neural Networks Configuration and Training

In the final solution, two different (symmetric and modified) MLFFNNs were trained and used for the prediction of loads. The architectures of both networks are presented in Fig. 3. The trainable parameters in both proposed implementations are located in dense layers only. This choice was made to take into account the possible connection between RCS values in different directions, which is especially valid for structures with symmetry of radiation patterns and low structural scattering. Both developed NNs have a separation for each load value prediction. The presence of dense layers before the separation on different branches reflects the fact of mutual influence of loaded antennas. At the same time, layers after the separation lead to the determination of each load independently. It follows the fact that the function of dependence between scattering and load for each antenna must differ in coupled cases due to the mutual influence on radiation patterns. Fig. 3 demonstrates that the modified MLFFNN has more layers to increase the sensibility of the prediction algorithm for small changes in the RCS. Moreover, one of the branches (for prediction of Load 1 value) has fewer neurons in its added, in comparison with the symmetric, layer. This decision was made due to observation during the training process of symmetric MLFFNN that the training of this branch has happened at a lower rate than those of the others.

For activation layers for each non-final dense layer, the leaky ReLu activation function was chosen to provide the possibility of a negative connection between neurons. However, the slope coefficient was equal to 0.1 to prevent a negative values in neurons of the last layers of the networks. Additionally, to prevent the overfitting of MLFFNNs, dropout layers with a rate equals to 0.1 after each ReLu layer were added.

The training process itself was done using Google Colab utilizing the Tensorflow library. Each MLFFNN was compiled using Adam optimizer with an initial learning rate equal to $LR_0 = 10^{-4}$ and $\epsilon = 10^{-6}$ with default values of other hyperparameters. The loss function was a sum of categorical cross-entropy losses for each output of the network. Categorical accuracy was metrics and was controlled separately for each load on each epoch of the training process. The whole fitting process had $E = 120$ epochs for each network with batch size equal to $bs = 3$ samples. Moreover, the learning rate for each epoch was equal to

$$LR_{ep} = 0.97^{(ep-1)} LR_0, \tag{1}$$

where ep is the number of the training epoch, to provide higher accuracy. To prevent overfitting, the early stopping mechanism was introduced. Its patience was equal to 5 epochs with control of the minimal value of the loss function on the validation data. However, in both cases, the fitting process was done until the last epoch without early stopping triggering.

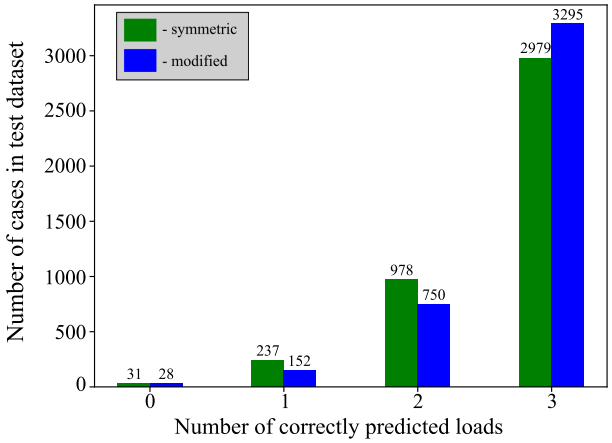

Fig. 4. Histogram disposing the number of correctly predicted load values on the test dataset by each MLFFNN under research.

TABLE II
VALUES OF CATEGORICAL ACCURACY ON THE LAST EPOCH

Network	Load	Dataset	Categorical accuracy
Symmetric	1	Train	0.5970
		Validation	0.7759
	2	Train	0.7670
		Validation	0.8998
	3	Train	0.7978
		Validation	0.9219
Modified	1	Train	0.6182
		Validation	0.8600
	2	Train	0.7916
		Validation	0.9243
	3	Train	0.8223
		Validation	0.9341

IV. RESULTS AND DISCUSSION

The results of the training process for both MLFFNNs under consideration are shown in Table II and in Fig. 4. Both describe the ability of the NNs to predict load values of the scattering system based on the provided not-known-before RCS data. It is possible to see that in both cases the number of totally correct predictions (all three loads determined correctly) is higher than 70.5% out of 4225 samples. Based on the accuracy values, the load of the first antenna is predicted with the worst rate. An application of the network with higher accuracy and equalization of the training complexity for all loads led to the increase of accuracy of the model and a faster decrease of loss function on the validation dataset during the fitting process. At the same time, accuracy values on validation sets for all loads and networks were higher than on train sets. It may indicate either a limitation in the resolution of validation datasets (due to a limited number of cases) or the possibility of continuing the MLFFNNs training process without overfitting. As a result, the developed MLFFNNs may with sufficient accuracy predict the load values based on the bistatic RCS pattern of the structure.

TABLE III
VALUES OF PREDICTED LOADS FROM THE FORMED DESIRED BISTATIC RCS PATTERNS IN DEFINED DIRECTIONS

Network	Desired direction	Load 1	Load 2	Load 3
Symmetric	$\phi = 0°$	5.1 nH	1 pF	1 pF
	$\phi = 40°$	0.9 nH	open	1 pF
	$\phi = 130°$	8 pF	50 Ω	50 Ω
	$\phi = 180°$	5.1 nH	1 pF	1 pF
	$\phi = 40°$ and $130°$	7 pF	open	1 pF
Modified	$\phi = 0°$	5.1 nH	1 pF	1 pF
	$\phi = 40°$	1 nH	open	50 Ω
	$\phi = 130°$	8 pF	open	50 Ω
	$\phi = 180°$	3 nH	1 pF	1 pF
	$\phi = 40°$ and $130°$	2 pF	open	1 pF

In the following step, the models were used for the prediction of load values from the desired RCS arrays. Due to the physical limitations of the considered structure, we decided to optimize RCS solely for azimuthal plane ($\theta = 90°$). The predictions of the trained models for the desired patterns are presented in Table III, while the CST Studio Suite simulations of bistatic RCS for all listed cases are illustrated in Fig. 5.

Several interesting observations may be made based on the received results. Firstly, both networks reshape the pattern trying to increase the RCS value in the defined direction in comparison with the reference case (50-Ω-termination). This fact provides the general usability of the proposed approach for optimization goals. Secondly, despite the higher accuracy on the test dataset, the modified MLFFNN in some cases provided weaker scattering in the required direction (for example, for $\phi = 40°$ and $\phi = 130°$ cases). However, taking into account the requirement of absence of scattering into other directions, the reason behind it is an attempt of the second network to reduce scattering into other directions. Thus, for $\phi = 130°$ case it is clearly visible from Fig. 5b that the structure main lobe maxima is directed towards $130°$, while the same point in Fig. 5a is closer to $180°$. At the same time, for the case of the identical direction of lobes, modified MLFFNN provides a higher RCS value in the maximized direction (for example, $\phi = 180°$ case). All these observations lead to the conclusion about the necessity of more thoughtful creation of the desired RCS array. Thus, structural scattering or unit antenna properties may be used in this process (in the current example, the fact of low scattering from the material of antennas itself and symmetry of dipoles' patterns could be utilized). Thirdly, for complicated radiation patterns with several main directions ($\phi = 40°$ and $130°$ case), both networks showed optimal results with a trend to equalization of scattering in both directions. It shows the possibility of the approach to optimize loads for several directions scattering simultaneously. Finally, the uncertainty of both models in the values of the first load of the structure may be used for the analysis of the influence of each load on bistatic RCS patterns.

Noticeable that the prediction based on the MLFFNNs may be not effective for some directions, especially in the case of

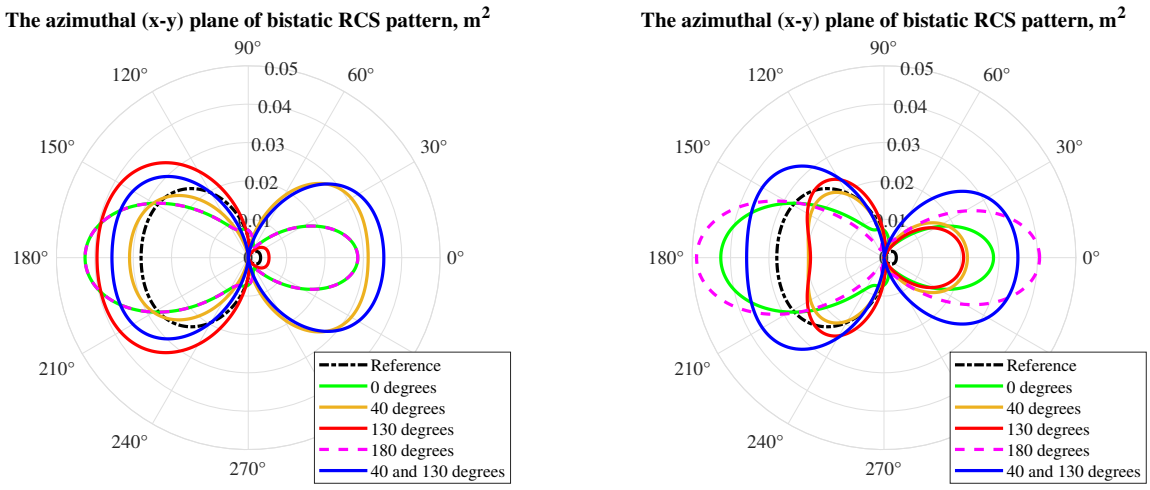

(a) Results for symmetric MLFFNN

(b) Results for modified MLFFNN

Fig. 5. Bistatic RCS patterns cuts for $\theta = 90°$ received based on the predictions made by trained MLFFNNs. The reference line describes the scattering of the system with termination of each antenna port to 50 Ω. All other lines indicates the result for the optimization of RCS in the corresponding direction.

small values of bistatic RCS in these directions (for example, $\phi = 90°$). Moreover, the potential increase of the number of loads necessitates the scaling of MLFFNNs through the addition of layers or neurons per layer. The expansion in the load value combinations will lead to a reduction of the proportion covered by the training dataset, while example networks were trained on 65% of all possible combinations of loads which may be hard to achieve in general cases. While the proposed method is applicable for optimizing real structures based on defined scattering properties, it is possible to introduce an update of weights of the higher layers based on the scattering system's operation results. For these reasons, the research of alternative machine learning-based approaches for optimization, including transition to regression tasks, could be done in future.

V. Conclusion

This paper proposes the method of the load values of antenna-based scattering system optimization using MLFFNN. The developed models demonstrate usefulness for the load values prediction based on the RCS patterns and could be applied in modifications of bistatic RCS patterns. The relative simplicity and scalability of the model allow its use for different types of antennas and a number of loads. Possible improvements can be made in future work, including redefinition of the desired RCS pattern utilizing scattering system properties, changing the task to regression, optimization of structural and antenna scattering modes separately, and consideration of structural parameters optimization partially using the same architecture of neural networks.

Acknowledgment

The research was partly funded by the WALLPAPER project of the Academy of Finland under decision 352913. The project utilized the Aalto Electronics-ICT infrastructure of Aalto University.

References

[1] Z. Niu, W. Ma, W. Wang, and T. Jiang, "Spatial modulation-based ambient backscatter: Bringing energy self-sustainability to massive internet of everything in 6G," *China Communications*, vol. 17, no. 12, pp. 52–65, 2020.

[2] M. D. Renzo, A. Zappone, M. Debbah, M.-S. Alouini, C. Yuen, J. de Rosny, and S. Tretyakov, "Smart radio environments empowered by reconfigurable intelligent surfaces: How it works, state of research, and the road ahead," *IEEE Journal on Selected Areas in Communications*, vol. 38, no. 11, pp. 2450–2525, 2020.

[3] H. E. Hassani, X. Qian, S. Jeong, N. S. Perović, M. D. Renzo, P. Mursia, V. Sciancalepore, and X. Costa-Pérez, "Optimization of RIS-aided MIMO – a mutually coupled loaded wire dipole model," unpublished.

[4] A. Abrardo, A. Toccafondi, and M. D. Renzo, "Analysis and optimization of reconfigurable intelligent surfaces based on S-parameters multiport network theory," unpublished.

[5] K.-C. Lee, "Application of neural network and its extension of derivative to scattering from a nonlinearly loaded antenna," *IEEE Transactions on Antennas and Propagation*, vol. 55, no. 3, pp. 990–993, 2007.

[6] Y. Wei, J. Li, and C. Gu, "Study on two-dimensional electromagnetic scattering based on BP neural network," in *2022 IEEE 4th International Conference on Civil Aviation Safety and Information Technology (ICCASIT)*, 2022, pp. 888–891.

[7] P. Liu and Z. N. Chen, "Full-range amplitude–phase metacells for sidelobe suppression of metalens antenna using prior-knowledge-guided deep-learning-enabled synthesis," *IEEE Transactions on Antennas and Propagation*, vol. 71, no. 6, pp. 5036–5045, 2023.

[8] C. Huang, G. Chen, J. Tang, P. Xiao, and Z. Han, "Machine-learning-empowered passive beamforming and routing design for multi-ris-assisted multihop networks," *IEEE Internet of Things Journal*, vol. 9, no. 24, pp. 25 673–25 684, 2022.

[9] Z. Wei, Z. Zhou, P. Wang, J. Ren, Y. Yin, G. F. Pedersen, and M. Shen, "Automated antenna design via domain knowledge-informed reinforcement learning and imitation learning," *IEEE Transactions on Antennas and Propagation*, vol. 71, no. 7, pp. 5549–5557, 2023.

[10] A. Gupta, E. A. Karahan, C. Bhat, K. Sengupta, and U. K. Khankhoje, "Tandem neural network based design of multiband antennas," *IEEE Transactions on Antennas and Propagation*, vol. 71, no. 8, pp. 6308–6317, 2023.

[11] G. Gradoni and M. Di Renzo, "End-to-end mutual coupling aware communication model for reconfigurable intelligent surfaces: An electromagnetic-compliant approach based on mutual impedances," *IEEE Wireless Communications Letters*, vol. 10, no. 5, pp. 938–942, 2021.

[12] B. Mirkin, *Core Concepts in Data Analysis: Summarization, Correlation and Visualization*. Springer London, 01 2011.